Astron. Astrophys. 331, 1051–1058 (1998)

ASTRONOMY
AND
ASTROPHYSICS

Research Note

The importance of collision broadening of weak lines in stellar spectra

Sean G. Ryan

[1] Royal Greenwich Observatory, Madingley Road, Cambridge CB3 0EZ, UK
[2] Anglo-Australian Observatory, P.O. Box 296, Epping NSW 2121, Australia

Received 11 July 1997 / Accepted 24 November 1997

Abstract. Several formalisms for computing the collision broadening of weak iron lines are compared. These include approximations to Van der Waals broadening, empirical enhancement factors, the WIDTH6 approximation, and the Anstee & O'Mara calculations. Abundances are computed for a set of red Fe I lines using solar data, to illustrate the effects of selecting one or other damping formalism. The main points of this research are:

1. even weak lines (log $(W/\lambda) = -5$) lacking strong wings are sensitive to the choice of damping, the abundances inferred from them varying by as much as 0.1 in dwarfs (but by less in giants) depending on the adopted formalism and excitation potential. In slightly stronger lines, having log $(W/\lambda) = -4.8$, the errors may reach 0.2 dex;
2. damping errors can depend strongly on both excitation potential and equivalent width, and could mislead an analyst into adopting an inappropriate effective temperature (in error by $\sim$100 K or more) and microturbulence. In particular, the WIDTH6 formalism is probably unsuitable for many optical lines having $\chi > 2$ eV.
3. the effects of an incorrect damping choice can be reduced, though not eliminated, by adjusting the microturbulence, but only for elements with many lines spanning a large range of equivalent widths. In practice, this restricts the adjustment to neutral iron lines, leaving the analysis of other species open to potentially large errors;
4. until reliable damping values are available for many lines of many species, the benefits of having high S/N spectra and gf values accurate to a few percent will seldom be realized in abundances accurate to a few $\times$0.01 dex;
5. the poor understanding of microturbulence and the need to quantify it empirically during an abundance analysis represent significant deficiencies in our understanding of stellar absorption line physics, and limit the accuracy of stellar abundances.

Send offprint requests to: S. Ryan (sgr@ast.cam.ac.uk)

Key words: line: formation – methods: data analysis – Sun: abundances – stars: abundances

1. Introduction

Detailed stellar abundance analyses have generally targeted weak lines lying on the linear portion of the curve of growth, where $\log(W/\lambda) \lesssim -5$, for W and λ the equivalent width and wavelength respectively. Weak lines have been favoured over stronger ones for a number of reasons including:

- their equivalent widths exhibit maximum sensitivity to abundance;
- they are less affected by the uncertain atmospheric parameters of microturbulence and gravity; and
- the broad "damping" wings of strong lines require that the collision broadening be known.

As the strengths of weak absorption lines reflect the opacity in the Doppler–dominated line core more–so than that in the Lorentzian wings, the sometimes–large uncertainties in collision broadening calculations have generally been regarded as unimportant in the analysis of weak lines. Some twenty–five years have passed since Blackwell, Calamai, & Willis (1972) discussed the effects of uncertainties in damping and microturbulence on abundance analyses, and it is over a decade and a half since Gurtovenko & Kondrashova (1980) reviewed available data on damping. In the meantime, high S/N spectra have become the norm and gf values accurate to within a few percent are more common, and greater accuracy is expected from stellar abundance analyses than might previously have been the case. In view of this, it is appropriate to revisit the issue of collision broadening of weak lines, and to be aware of lingering uncertainties in this aspect of an abundance analysis. It is the purpose of this *Research Note* to draw attention again to the importance

of collision broadening even for weak lines, and to highlight the consequences of adopting various formalisms for computing it.

The paper is set out as follows. In Sect. 2, collision broadening is discussed in general terms, followed in Sect. 3 by a description of several collision broadening formalisms. In Sect. 4, damping widths are computed for a set of lines according to different prescriptions, and abundances are computed and discussed for several of these cases in Sect. 5, using solar data as the illustration.

2. Collision broadening

Once thermal broadening and microturbulence are taken into account, the mechanism responsible for broadening the majority of metallic lines in the spectra of solar–type stars is collisions with neutral hydrogen. In an abundance analysis, it has been common to compute the collision broadening using some approximation to Van der Waals interaction, but it has long been recognised that the broadening so derived is too weak. Enhancements to the damping width γ by factors between 1.0 and 5.0 have often been applied (e.g. Holweger 1971, Gurtovenko & Kondrashova 1980 (esp. Table IA), Simmons & Blackwell 1982).

The shaky foundation provided by approximations to the Van der Waals interaction is highlighted in several works. The interaction potential between an atom and it perturber is usually approximated by only the first term ($1/R^6$) in a $1/R$ expansion, but Roueff & Van Regemorter (1971; also Roueff 1975, Van Regemorter 1973) conclude that short–range rather than long–range interactions are important for broadening at stellar temperatures, questioning the validity of the $1/R^6$ expansion. Moreover, O'Mara & Gietzel (1978) demonstrated that the $1/R$ series expansion is formally divergent, and that for the short range interactions relevant to collisional broadening in stars, even the first term, $1/R^6$, contains large enough errors to render the approach unsuitable.

Despite these serious challenges to the validity of the Van der Waals interaction as the broadening *mechanism* for metallic lines, its ability to provide a value for the damping in error by an almost uniform factor for many lines (e.g. Holweger 1971) has resulted in the *formalism* surviving for several decades. Its retention has no doubt been encouraged by the lack of a better alternative for computing the broadening for large numbers of transitions. This last reason may have passed in the wake of recent work by Anstee & O'Mara (1995) and Barklem & O'Mara (1997) discussed below.

3. Collision broadening formalisms

Under the Van der Waals interaction, the interaction constant C_6 for an ion making the transition between states lo and hi and its H perturber is computed as

$$C_6 = \frac{\alpha e^2}{h}(\langle r_{hi}^2\rangle - \langle r_{lo}^2\rangle),$$

where $\langle r_i^2\rangle$ is the mean square radius of excitation state i in cm, α is the polarizability of the H atom, e is the electronic charge, and h is Planck's constant (e.g. Woolley & Stibbs 1953, Eq. (IX-45)). Expressing the mean square radii as R^2 in Bohr radii^2 (a_0^2) rather than r^2 in cm^2 gives

$$C_6 = 6.46 \times 10^{-34}(\langle R_{hi}^2\rangle - \langle R_{lo}^2\rangle). \quad (1)$$

Once the interaction constant is obtained, the damping per perturber can be computed as

$$\gamma_6/N_{\rm H} = 17\ C_6^{2/5} v^{3/5} \qquad \text{rad s}^{-1}$$

where v = average relative velocity of the atom and perturber (Unsöld 1955, Eq. (82,48); Gray 1992, Eq. (11.31,34)).

Most of the variety amongst computations of collision broadening arises in the approximation used for computing the mean square radii of the levels. Several of these are described below.

3.1. Scaled hydrogenic approximation

The scaled hydrogenic approximation for the mean square radius of excitation state i is

$$\langle R_i^2\rangle = \frac{n^{*2}}{2Z^2}\{5n^{*2} + 1 - 3l(l+1)\}$$

where Z is the effective nuclear charge seen by the electron (1 for Fe I, 2 for Fe II, etc.), l is the orbital angular momentum quantum number of state i, and n^* is the effective principal quantum number given by

$$n^{*2} = \frac{13.6Z^2}{I-\chi},$$

I being the ionisation energy of the atom (in eV), and χ the excitation energy of the state (in eV) (e.g. Woolley & Stibbs 1953, Eq. (IX-48)).

3.2. Unsöld's approximation

A widely adopted approximation is that due to Unsöld (1955), which differs from the hydrogenic approximation by not retaining the term $1 - 3l(l+1)$. This has the computational advantage that one no longer needs to know the orbital angular momentum quantum number l, and can compute the mean square radius of a state for essentially any line, needing to know only its excitation energy, ionisation energy, and ionisation state (which gives the effective nuclear charge).

3.3. Simmons & Blackwell enhancement

Based on fits to the wings of strong lines with accurately known gf values, Simmons & Blackwell (1982) derived the damping coefficients of a number of neutral iron lines empirically, and determined what enhancements were required to Unsöld's formalism. Their enhancements to γ ranged from 1.0 to 1.5, being higher in general for higher excitation levels. In the present work, $E_\gamma = 1.0 + 0.15\chi_{lo}$ is used as an approximation to the Simmons & Blackwell result.

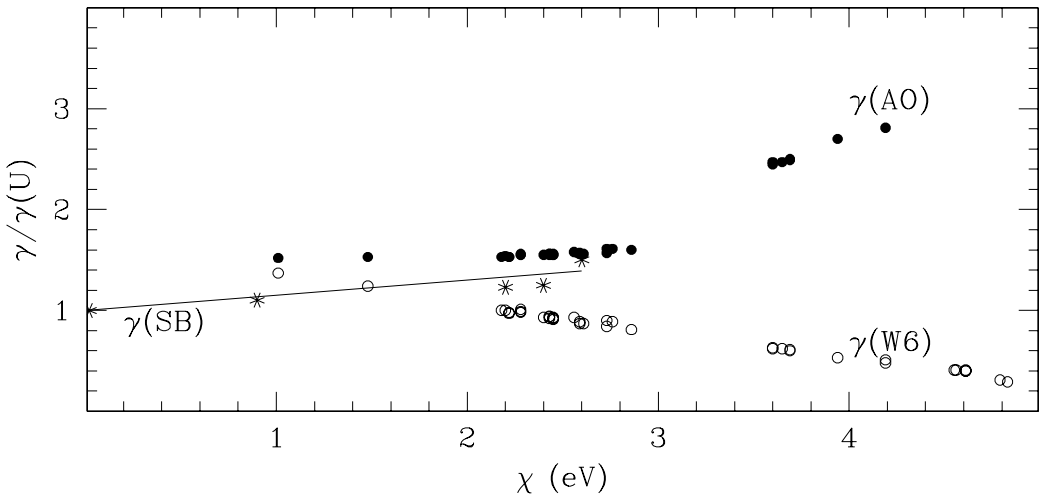

Fig. 1. Ratios of damping values computed by various formalisms: γ(Anstee & O'Mara)/γ(Unsöld) (*solid circles*), and γ(WIDTH6)/γ(Unsöld) (*open circles*). The asterisks and solid line show the empirical enhancement factors of Simmons & Blackwell and the linear approximation adopted here.

3.4. WIDTH6 approximation for the iron peak elements

Kurucz's WIDTH6 program is widely used for computing the abundances of stellar absorption lines. The approximation used there for lines in the iron peak elements (scandium to nickel inclusive), based on Kurucz's own computations of wavefunctions, is

$$\langle R^2_{hi} \rangle = \frac{45 - S}{Z}$$

where S is the number of electrons in the ion under consideration. Furthermore, WIDTH6 neglects the lower level entirely, adopting $\langle R^2_{hi} \rangle >> \langle R^2_{lo} \rangle$. This approach is retained in WIDTH9 (Kurucz 1993).

This approximation differs considerably from those presented earlier. It needs to be borne in mind that Kurucz was motivated to compute synthetic spectra of strong lines of the iron group whose upper states were 4p (Kurucz & Furenlid 1979). Consequently his approximation was tailored to these strong lines for which broadening clearly mattered, rather than to much weaker lines.

3.5. Anstee & O'Mara formulation

An alternative formulation by Brueckner (1971), which retains the full interaction potential rather than treating it as a series expansion in $1/R$, was developed further by O'Mara (1976) and Anstee & O'Mara (1991). Anstee & O'Mara (1995) have now computed the broadening cross sections for s-p and p-s transitions, tabulating these for a large range of quantum numbers.[1,2]

An application of those results led Anstee, O'Mara & Ross (1997) to derive a solar iron abundance matching the meteoritic value.

Anstee, O'Mara & Ross argue the value of using strong (damped) lines *in preference to* weak lines for abundance analyses once the broadening is known, since strong line wings are not sensitive to microturbulence or NLTE effects in line cores, and because of the relative ease of measuring strong lines. The last of these depends on the degree of line blending and on the reliability of the continuum placement. Despite these advantages, the absence of strong lines for many elements, especially in metal poor stars, means that weak–line analyses will retain their importance.

4. Calculations of damping for a sample of lines

To illustrate the effects of adopting the different broadening computations discussed in Sect. 3, damping widths and abundances were calculated for a set of red Fe I lines. The line list is given in Table 1, with the wavelengths and lower excitation potentials in columns (1) – (2). The angular momentum quantum numbers of the initial and final states are listed in column (5).

The mean square radii of the final and initial states are given in Bohr radii[2], firstly for the hydrogenic approximation (columns 6–7) and secondly for the Unsöld approximation (columns 8–9). Recall that C_6 depends on the difference between the final and initial values (Eq. (1)). In comparison, WIDTH6 adopts a single value for all Fe I transitions — 19 a_0^2 — and one value for all Fe II transitions — 10 a_0^2.

Columns (10) – (14) give the damping values log ($\gamma/N_{\rm H}$) computed for the five formalisms described in Sect. 3, for a temperature of 5000 K, which is typical of the atmospheres of G–K stars. Ratios of the γ values for various pairs of formalisms

[1] The expression $\gamma_6/N_{\rm H}$ = 17 $C_6^{2/5} v^{3/5}$ leads to a $\gamma \propto T^{2/5}$ relationship. However, the dependence that emerges from the Brueckner formalism has a slightly different *and non–universal* power, in the range $T^{0.3}$ to $T^{0.4}$. Anstee & O'Mara also tabulate the new powers.

[2] Tabulations for p-d and d-p transitions will be published imminently (Barklem & O'Mara 1997).

are given in columns (15) – (19). Three of these ratios are plotted in Fig. 1.

Fig. 1 shows that the WIDTH6 approach resembles the Unsöld approximation for lines around 2 eV. Recalling that Kurucz's motivation was to fit strong, low–excitation–potential lines, we see that WIDTH6 provides values for them comparable with mild enhancements ($E_\gamma \simeq 1.2 - 1.4$) of Unsöld's approximation. However, considerably larger differences exist for the higher excitation potential lines, where WIDTH6 values are a factor of two lower than Unsöld's. Presumably this difference arises because Kurucz's treatment is based on a 4p excited state, which is not appropriate for all Fe I lines.

Fig. 1 also compares the Anstee & O'Mara damping values with those of Unsöld. The Anstee & O'Mara calculations correspond to mild enhancements of the Unsöld values for lower excitation potential lines, consistent with empirical results, but gives higher enhancements $E_\gamma \simeq 2.5 - 3$ for lines around 4 eV. The Anstee & O'Mara γ values differ considerably from the WIDTH6 ones for lines above 2 eV, differing by a factor of 5 at 4 eV. Also shown in the figure are the empirical enhancement factors of Simmons & Blackwell (crosses) and the linear approximation (solid line) adopted for the calculations in Table 1.

5. The sensitivity of weak lines to collision damping

Having illustrated the differences between these damping formalisms, we now examine their effects on abundance computations. Equivalent widths were measured for each of these lines from the solar flux atlas of Beckers, Bridges & Gilliam (1976). The log gf values and equivalent widths are given in columns (3–4) of Table 1. Oscillator strengths for approximately half of the lines come from the highly accurate laboratory values by O'Brian et al. (1991), Bard, Kock & Kock (1991), Bard & Kock (1994), Blackwell, Petford & Simmons (1982b), and Blackwell et al. (1982a). The remainder are empirical values from Thévenin's (1990) solar analysis, or of mixed pedigree from the compilation by Fuhr, Martin & Wiese (1988).

Abundances were computed for four cases, using the Holweger–Muller solar model:

1. adopting Unsöld's approximation;
2. enhancing Unsöld's γ by a factor of 2.5, following Gurtovenko & Kondrashova (1980);
3. using the WIDTH6 approximation; and
4. using the Anstee & O'Mara formulation.

The computations were conducted using WIDTH6, but with the γ values described above.

The abundances obtained with microturbulence ξ = 1.0 km s^{-1} are plotted in the left–hand panels of Fig. 2 as a function of equivalent width.[3] The top panel shows that pure Unsöld's damping gives a uniform abundance for all of these weak lines. However, enhancing the damping by a factor 2.5 leads to a strong dependence on equivalent width, *even though these are "weak" lines.* Trends of varying slope also result from the other damping treatments. Linear least–squares fits were computed for each set of results, and are shown in the figure. The first result of this investigation can be stated:

– *even weak lines having log* $(W/\lambda) = -5$ *(i.e.* $W \simeq 65$ *mÅ in these red spectra) are affected by the choice of damping, by as much as 0.1 dex for a factor 2.5 change in damping.*

As already shown by Blackwell et al. (1972, Fig. 1(a)), the size of the abundance error resulting from a given damping error depends on the excitation potential of the line, lower excitation potential lines being the least sensitive.

When the weak lines of an element give abundances that depend on equivalent width, it is usually interpreted as a requirement for a different microturbulence, since this affects stronger lines more (e.g. Gray 1992, Fig. 14.4). Viewed simplistically, revision of the microturbulence has the effect of skewing the abundance trend about the exceptionally weak lines (W $\approx$ 0), and is equivalent to forcing their abundance on the other lines. It is clear from the convergence of the four trends at the y–axis that the error in the inferred mean iron abundance due to uncertainties in damping can be minimized *provided* the trends are eliminated by an alternative choice of microturbulence. Consequently, however, the derived microturbulence depends on the adopted damping treatment.

The central panels of Fig. 2 show the abundances resulting from alternative choices of microturbulence that reduce the trends for lines with $W < 100$ mÅ. (The abundances for ξ = 1 km s^{-1} are shown as open circles.) They illustrate that the "skewing" about $W = 0$ only occurs for lines weaker than about 150 mÅ, since lines of 200 mÅ (and stronger) are core–saturated and less sensitive to small changes of Doppler broadening in their cores. Thus, although the errors in an iron line analysis can be reduced by the microturbulence–damping trade–off, they cannot be completely eliminated, and it is not obvious that the microturbulence value used will be appropriate to the analysis of other elements (see below). Furthermore, errors as high as 0.1 or even 0.2 dex remain for lines around $W \sim 100-120$ mÅ.

A notable feature of Fig. 2 is that the scatter of the data about the trends is greater for the WIDTH6 formalism than for the other three. The nature of this is revealed in the right–hand panels, where the abundances derived using the WIDTH6 formalism are seen to depend strongly on excitation potential. This is exactly the behaviour to be expected based on the analysis of Fig. 1. There it was shown that WIDTH6 uses much lower damping values for the higher excitation potential lines than other formalisms do, by a factor of two compared with Unsöld and a factor of five compared with Anstee & O'Mara. There are two reasons for mistrusting the WIDTH6 values for the higher excitation potential line. Firstly, there is no reason to believe that these lines should have the same damping values as the strong lines to which Kurucz tailored his formalism. Secondly, empirical studies have generally shown that even Unsöld's values are too small, let alone finding acceptable values a factor of

[3] The physics of line transfer dictates that W/λ rather than W is the crucial value. However, since all of the lines here are confined to a small range in λ, use of W as the abscissa is quite acceptable. Observers seeking to generalize these results to some other wavelength λ_1 (Å) should multiply the equivalent widths quoted here by $\lambda_1/6500$.

Table 1. Sample list of red Fe I and Fe II lines

λ	χ_{lo}	log gf	$W_\odot$	l	$\langle R^2\rangle_{\rm hyd}$		$\langle R^2\rangle_{\rm U55}$		log ($\gamma/N_{\rm H}$)					γ ratios				
Å	eV		mÅ	lo-hi	hi	lo	hi	lo	hyd.	U55	W6	SB82	AO96	$\frac{\rm U55}{\rm hyd.}$	$\frac{\rm W6}{\rm U55}$	$\frac{\rm SB82}{\rm U55}$	$\frac{\rm AO96}{\rm W6}$	$\frac{\rm AO96}{\rm U55}$
(1)	(2)	(3)	(4)	(5)	(6)	(7)	(8)	(9)	(10)	(11)	(12)	(13)	(14)	(15)	(16)	(17)	(18)	(19)
Fe I																		
6102.18	4.83	-0.26	83	1-2	340	39	454	50	-7.44	-7.39	-7.92	-7.15	...	1.13	0.29	1.72	...	...
6136.62	2.45	-1.41	140	0-1	30	17	40	16	-7.99	-7.88	-7.92	-7.74	-7.69	1.28	0.91	1.37	1.70	1.55
6137.70	2.59	-1.38	133	0-1	33	18	43	17	-7.96	-7.86	-7.92	-7.72	-7.67	1.26	0.87	1.39	1.79	1.56
6170.49	4.79	-0.44	83	1-2	295	38	403	49	-7.47	-7.41	-7.92	-7.18	...	1.14	0.31	1.72	...	...
6173.34	2.22	-2.88	69	0-1	25	16	35	14	-8.04	-7.91	-7.92	-7.79	-7.73	1.34	0.97	1.33	1.57	1.53
6180.22	2.73	-2.62	56	0-1	36	19	47	17	-7.94	-7.85	-7.92	-7.70	-7.65	1.24	0.84	1.41	1.87	1.57
6188.04	3.94	-1.72	48	1-0	128	21	124	30	-7.62	-7.64	-7.92	-7.44	-7.21	0.95	0.53	1.59	5.13	2.70
6191.57	2.43	-1.38	132	0-1	29	17	39	16	-8.00	-7.89	-7.92	-7.75	-7.70	1.29	0.92	1.36	1.68	1.55
6200.32	2.61	-2.41	73	0-1	33	18	43	17	-7.96	-7.86	-7.92	-7.72	-7.67	1.26	0.87	1.39	1.79	1.56
6240.66	2.22	-3.20	49	0-1	25	16	34	14	-8.04	-7.91	-7.92	-7.79	-7.73	1.35	0.98	1.33	1.56	1.53
6246.32	3.60	-0.81	125	1-0	91	17	88	25	-7.69	-7.71	-7.92	-7.53	-7.32	0.94	0.62	1.54	3.98	2.47
6252.55	2.40	-1.73	121	0-1	28	17	38	15	-8.01	-7.89	-7.92	-7.76	-7.70	1.31	0.93	1.36	1.66	1.55
6256.37	2.45	-2.41	95	0-1	29	17	39	16	-8.00	-7.89	-7.92	-7.75	-7.70	1.30	0.92	1.37	1.69	1.55
6265.13	2.18	-2.55	86	0-1	24	15	34	14	-8.05	-7.92	-7.92	-7.80	-7.74	1.36	1.00	1.33	1.54	1.53
6270.24	2.86	-2.54	54	0-1	39	20	50	18	-7.92	-7.83	-7.92	-7.68	-7.63	1.22	0.81	1.43	1.96	1.60
6318.03	2.45	-2.00	106	0-1	29	17	39	16	-8.00	-7.89	-7.92	-7.75	-7.70	1.30	0.93	1.37	1.68	1.56
6322.69	2.59	-2.45	77	0-1	32	18	42	17	-7.98	-7.87	-7.92	-7.73	-7.68	1.27	0.89	1.39	1.76	1.57
6335.34	2.20	-2.18	99	0-1	24	16	33	14	-8.06	-7.92	-7.92	-7.80	-7.73	1.37	1.00	1.33	1.54	1.54
6336.84	3.69	-0.86	113	1-0	96	18	93	26	-7.68	-7.70	-7.92	-7.51	-7.31	0.94	0.60	1.55	4.13	2.50
6344.15	2.43	-2.90	59	0-1	28	17	38	16	-8.01	-7.89	-7.92	-7.76	-7.70	1.31	0.94	1.36	1.66	1.56
6380.75	4.19	-1.38	52	2-1	133	3	153	34	-7.59	-7.60	-7.92	-7.39	...	0.96	0.48	1.63	...	...
6392.55	2.28	-4.03	18	0-1	25	16	35	15	-8.05	-7.91	-7.92	-7.79	-7.72	1.35	0.98	1.34	1.58	1.55
6393.60	2.43	-1.50	135	0-1	28	17	38	16	-8.02	-7.90	-7.92	-7.76	-7.70	1.32	0.94	1.36	1.66	1.56
6400.00	3.60	-0.29	200	1-0	88	17	85	25	-7.69	-7.72	-7.92	-7.54	-7.34	0.94	0.63	1.54	3.86	2.45
6408.03	3.69	-1.02	99	1-0	95	18	92	26	-7.68	-7.71	-7.92	-7.52	-7.31	0.94	0.61	1.55	4.08	2.49
6411.65	3.65	-0.66	135	1-0	91	18	88	26	-7.69	-7.72	-7.92	-7.53	-7.32	0.94	0.62	1.55	3.98	2.47
6421.36	2.28	-1.98	113	0-1	25	16	34	15	-8.05	-7.92	-7.92	-7.79	-7.73	1.36	0.99	1.34	1.57	1.55
6608.03	2.28	-4.03	19	0-1	24	16	33	15	-8.07	-7.93	-7.92	-7.80	-7.73	1.38	1.01	1.34	1.55	1.56
6609.12	2.56	-2.68	69	0-1	29	18	39	16	-8.01	-7.89	-7.92	-7.75	-7.69	1.31	0.93	1.38	1.70	1.58
6625.04	1.01	-5.35	17	0-1	12	11	19	10	-8.44	-8.06	-7.92	-8.00	-7.88	2.44	1.37	1.15	1.11	1.52
6627.56	4.55	-1.68	30	1-0	225	32	220	42	-7.52	-7.53	-7.92	-7.31	...	0.97	0.41	1.68	...	...
6633.76	4.56	-0.80	68	1-2	142	32	222	42	-7.62	-7.53	-7.92	-7.31	...	1.22	0.41	1.68	...	...
6703.57	2.76	-3.16	38	0-1	33	19	43	18	-7.98	-7.87	-7.92	-7.72	-7.66	1.28	0.89	1.41	1.81	1.61
6710.31	1.48	-4.88	17	0-1	15	12	22	11	-8.27	-8.02	-7.92	-7.93	-7.83	1.81	1.24	1.22	1.23	1.53
6715.41	4.61	-1.64	27	1-0	236	33	231	43	-7.51	-7.52	-7.92	-7.30	...	0.97	0.40	1.69	...	...
6726.67	4.61	-1.12	47	1-2	148	33	230	43	-7.61	-7.53	-7.92	-7.30	...	1.21	0.40	1.69	...	...
6786.88	4.19	-2.07	25	1-0	138	25	134	34	-7.61	-7.63	-7.92	-7.42	-7.18	0.95	0.51	1.63	5.46	2.81
6806.85	2.73	-3.21	34	0-1	32	19	42	17	-7.99	-7.88	-7.92	-7.73	-7.67	1.29	0.90	1.41	1.78	1.61
6810.27	4.61	-0.99	51	1-2	143	33	223	43	-7.62	-7.53	-7.92	-7.30	...	1.22	0.41	1.69	...	...
Fe II																		
6238.39	3.89	-2.87	47	0-1	14	13	17	12	-8.38	-8.15	-8.03	...	...	1.72	1.30	...	...	...
6247.55	3.89	-2.51	54	0-1	14	13	17	12	-8.38	-8.15	-8.03	...	...	1.72	1.30	...	...	...
6416.93	3.89	-2.85	41	0-1	14	13	17	12	-8.41	-8.15	-8.03	...	...	1.79	1.32	...	...	...
6456.39	3.90	-2.30	65	0-1	14	13	17	12	-8.41	-8.15	-8.03	...	...	1.80	1.32	...	...	...

two lower. For these reasons, it is the author's opinion that the higher excitation potential lines are inappropriately treated by WIDTH6. As a result of the broadening being too low, the program must infer higher abundances than for the lower excitation potential lines. A similar trend, though to a lesser degree, may also be seen for the pure Unsöld case, but not for the Anstee & O'Mara analysis.

As a related caution, it is noted that trends of abundance with excitation potential are often regarded as a reason for adjusting the adopted effective temperature. For the sun, a slope of 0.02 dex $\rm eV^{-1}$ could be eliminated by a temperature change of +100 K. However, following such a procedure for the data in the right hand panel of Fig. 2 would obviously be wrong. If it were applied, the pure Unsöld calculation would suggest a temperature increase of order 300 K, and the WIDTH6 data would suggest a change twice as great. It needs to be remembered, then, that errors in the microturbulence–damping trade–off (which depend on W) will also vary with excitation potential, and will mislead attempts to derive effective temperatures based on trends with χ. Potential errors, if the damping is not known accurately, certainly reach into the realm of 100 K or more. Recall in addition that the abundance error induced by a

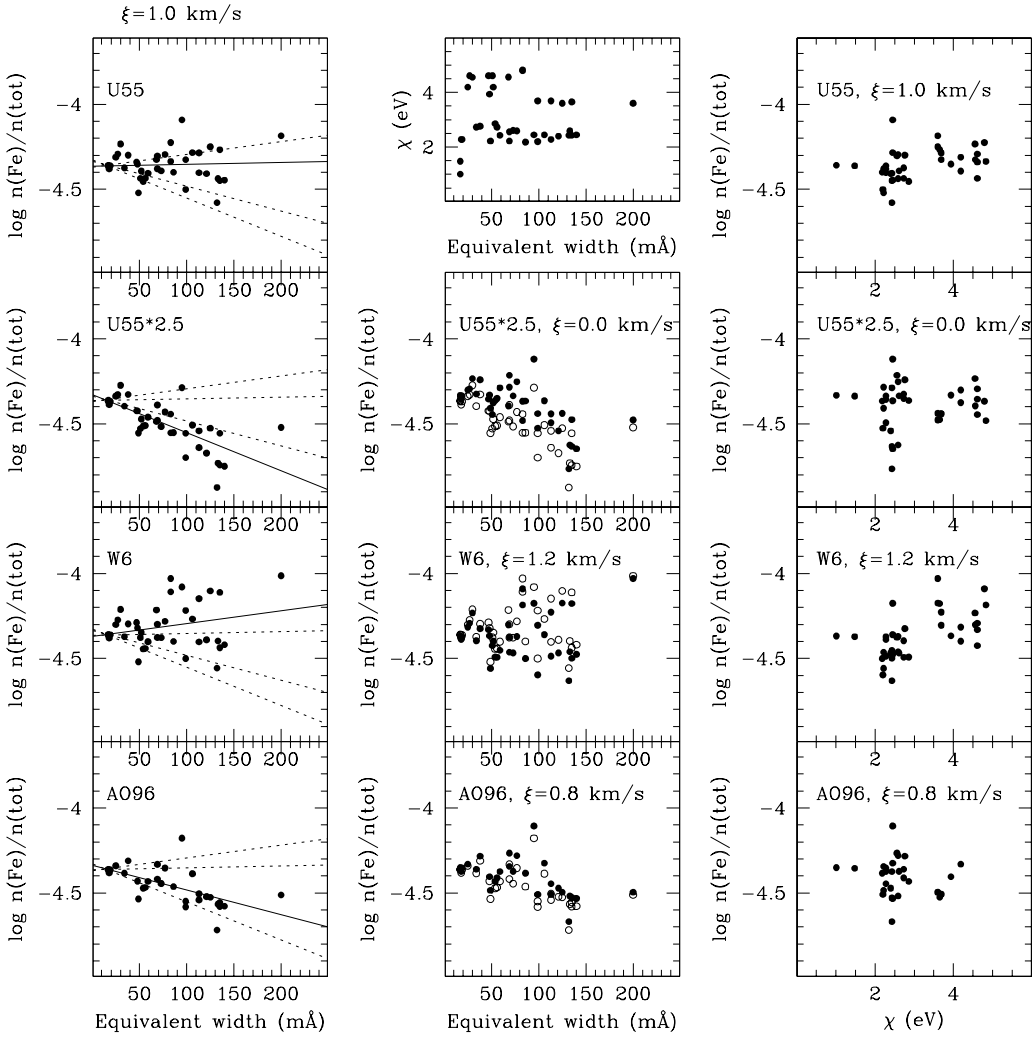

Fig. 2. Abundances, as a function of equivalent width, for red Fe I lines in the sun, for four different damping formalisms.
Left–hand panels: assuming microturbulence ξ = 1.0 km s^{-1}. Least–squares fits are shown, with the fit for the data in a given panel shown as a solid line.
Central panels: the microturbulence has been adjusted in each case to the value shown, to reduce the dependence of abundance on equivalent width for lines with $W < 100$ mÅ. The abundances from the left–hand panels are shown as open circles. No attempt has been made to adjust ξ for the case of pure Unsöld damping, as the trend has minimal slope. The mixture of excitation potentials and line widths in the sample is shown in the inset.
Right–hand panels: The abundances for the four cases are also found to depend on excitation potential, due to the dependence of damping errors on χ. The high excitation potential lines in the WIDTH6 formalism are believed to be least trustworthy (see text).

given damping error also depends on χ (Blackwell et al. 1971, Fig. 1).

The second key result of this paper may be stated:

– *errors induced by incorrect damping can be strongly dependent on excitation potential, not just equivalent width, and could mislead an analyst into adopting an effective temperature in error by ∼100 K or more. In particular, the WIDTH6 formalism as applied to high excitation potential lines is viewed with mistrust.*

Other elements can be more susceptible to residual errors. Particularly in metal poor stars, there are seldom enough lines with good gf values and spanning a wide range in equivalent width to permit the microturbulence to be redetermined, and the conventional practice is to adopt the microturbulence based on the neutral iron lines. However, the iron–based microturbulence is affected by the iron damping formalism, and it is not clear that the same microturbulent value or damping formalism will be appropriate for other elements. The influence of microturbulence also depends on atomic mass; microturbulence dominates the line–core broadening for heavy atoms, but is less important for species lighter than iron where thermal broadening is more important. Other elements suffer from two further difficulties. It is rarely possible to base an abundance measurement solely on very weak ($W/\lambda << -5$) lines that have been measured

reliably, and nor do they usually have large numbers of lines spanning a wide range of equivalent widths to verify that abundance trends have been eliminated. The sizes of the residuals in the central (ξ–adjusted) panels of Fig. 2 suggest that even if the same parameters as for Fe I were appropriate, systematic errors of 0.1 dex could remain for individual lines around 100 mÅ. The third key result of this paper is:

– *even though changes in microturbulence may reduce the severity of errors induced by incorrect damping, it cannot completely compensate. Furthermore, most elements lack large numbers of lines spanning a wide range of equivalent widths, so residual systematic errors which could be as large as 0.1 or even 0.2 dex will go unnoticed and uncorrected.*

It should be noted that the impact of damping errors also depends on evolutionary state. As giants typically have higher microturbulence — $\xi \sim 1.5 - 2.5$ km s^{-1} — than dwarfs — $\xi \sim 1.0 - 1.5$ km s^{-1} — the absorption lines in the giants will have broader Doppler cores and will therefore be less sensitive to errors in γ for the same equivalent width.

One of the benefits of deriving metal abundances relative to iron is that many systematic errors are minimised, so [X/Fe] is generally known more reliably than [Fe/H]. However, since the errors induced by incorrect damping and/or microturbulence depend on line strength, they will not cancel. Furthermore, if two stars have sufficiently different equivalent widths for a given line set, then the size of the error will also differ from star to star. Only when almost identical stars are compared will the errors be the same in each one.

The interdependency of microturbulent velocity and damping enhancement highlights the need to consider whether the practice of adjusting ξ to eliminate equivalent width dependences has obscured the flaws in our understanding of the real physics of spectral line formation. Improved understanding of microturbulence is unlikely to overhaul models of galactic chemical enrichment, but as atomic and observational data reach unprecedented levels of accuracy, it is worth remembering that our understanding of stellar line formation is still incomplete, and that abundances accurate to a few $\times$0.01 dex are unlikely to be possible without overcoming these deficiencies.[4]

The final two conclusions of this work may be stated:

– *although high S/N spectra and gf values accurate to a few percent are now common, the routine determination of abundances accurate to a few $\times$0.01 dex will not be possible until reliable damping values are available for many lines of many species;*
– *the poor understanding of microturbulence and the need to quantify it empirically during an abundance analysis represent significant deficiencies in our understanding of stellar absorption line physics, and limit the accuracy of stellar abundance measurements.*

6. A note on differences in coding

All computations presented in this work have been based on a unix implementation of WIDTH6. Computations for a particular test line (Fe I 5247) were also made using two additional codes. One was a unix implementation of the spectrum synthesis program of Cottrell (Cottrell & Norris 1978), and the second was the PC code of Ross (1997)[5]. As this line has a very low excitation potential, it is only weakly sensitive to damping, but nevertheless ought to give the same sensitivity to line broadening irrespective of which code is used. Regrettably, this is not the case. Calculations were performed for the solar line strength in a Holweger–Müller model using ξ=0.85 km s^{-1}. When pure Unsöld damping was used in both programs, Cottrell's gave an iron abundance lower than WIDTH6 by only 0.007 dex; i.e. in good agreement. The Ross code gave an abundance 0.019 dex lower than WIDTH6, but as it's damping implementation ignores the inner level, this difference is of minor concern. More disturbing, however, was the result when γ_6 was enhanced by a factor of 2.0. The resulting abundance change was 0.062 dex for WIDTH6, but only 0.043 dex for the Cottrell code and 0.038 dex for the Ross code.

The origin of the difference between the WIDTH6 and Cottrell implementations is unclear. As the sensitivity given by WIDTH6 differs from that found with the Cottrell code by a factor of 1.4 for the particular Fe I line tested, it raises the possibility that the differences shown earlier in this paper might be upper limits on the extent of the errors. However, even scaling down the size of the errors will not undermine the main results of this work, which is that weak lines are *not* immune to the effects of uncertain damping, that the errors can be strongly dependent upon equivalent width and excitation potential, and that efforts to exploit high S/N spectra utilising accurate gf values may ultimately be limited by errors in the adopted damping values and (relatedly) in our characterisation of microturbulence. Errors in the model atmospheres must also be considered.

Acknowledgements. It is a pleasure to acknowledge fruitful discussions with Drs M. S. Bessell, S. Feltzing, J. E. Norris, and B. J. O'Mara on these issues.

References

Anstee, S. D. & O'Mara, B. J. 1991, MNRAS, 253, 549
Anstee, S. D. & O'Mara, B. J. 1995, MNRAS, 276, 859
Anstee, S. D., O'Mara, B. J., & Ross, 1997, MNRAS, 284, 202
Bard, A., Kock, A., & Kock, M. 1991, A&A, 248, 315
Bard, A. & Kock, M. 1994, A&A, 282, 1014
Barklem, P. S. & O'Mara, B. J. 1997, MNRAS, in press
Beckers, J. M., Bridges, C. A. & Gilliam, L. B. 1976, A High Resolution Spectral Atlas of the Solar Irradience from 380 to 700

[4] Lithium, being such a light element, is dominated by thermal broadening, and is consequently insensitive to variations of its collisional damping by a factor of two or so. For the same reason, it is insensitive to variations in microturbulence and is one of the few elements for which abundances can be derived to a few $\times$0.01 dex, provided other sources of error can be restricted.

[5] The PC computations were kindly performed by Dr B. J. O'Mara and J. E. Ross.

nanometers. Volume I. Tabular Form (Air Force Geophysics Lab, Massachusetts)
Blackwell, D. E., Calamai, G., & Willis, R. B. 1972, MNRAS, 160, 121
Blackwell, D. E., Petford, A. D., Shallis, M. J., & Simmons, G. J . 1982a, MNRAS, 199, 43
Blackwell, D. E., Petford, A. D., & Simmons, G. J. 1982b, MNRAS, 201, 595
Brueckner, K. A. 1971, ApJ, 169, 621
Fuhr, J. R., Martin, G. A., & Wiese, W. L. 1988, J.Phys.Chem.Ref. Data, 17, Suppl. 4
Gurtovenko, E. A. & Kondrashova, N. N. 1980, Sol.Phys., 68, 17
Holweger, H. 1971, A&A, 10, 128
Holweger, H. & Müller, E. A. 1974, Sol.Phys., 39, 19
Kurucz, R. L. 1993, CDROM 13, (SAO, Cambridge)
Kurucz, R. L. & Furenlid, I. 1979, SAO Special Report 387, Sample Spectral Atlas for Sirius, (SAO, Cambridge)
O'Brian, T. R., Wickliffe, M. E., Lawler, J. E., Whaling, W., & Brault, J. W. 1991, J.Opt.Soc.Am.B., 8, 1185
O'Mara, B. J. 1976, MNRAS, 177, 551
O'Mara, B. J. & Barklem, 1997, MNRAS, preprint
O'Mara, B. J. & Gietzel, P. C. 1978, MNRAS, 184, 205
Ross, J. E. 1997, http://www.uq.edu.au/~phjross/
Roueff, E. 1975, A&A, 38, 41
Roueff, E. & Van Regemorter, H. 1971, A&A, 12, 317
Simmons, G. J. & Blackwell, D. E. 1982, A&A, 112, 209
Thévenin, F. 1990, A&AS, 82, 179
Unsöld, A. 1955, Physik der Sternatmosphären, (Springer–Verlag, Berlin)
Van Regemorter, H. 1973, Reports on Astronomy, Trans. IAU, 15A, C. De Jager, ed, (Reidel, Dordrecht), 155
Woolley, R. v. d. R., & Stibbs, D. W. N. 1953, The Outer Layers of a Star, (Oxford Uni. Press, London)

This article was processed by the author using Springer-Verlag LaTeX A&A style file *L-AA* version 3.